SERS-Based Sensing in Vitro: Facile and Label-Free Detection of Apoptotic Cells at the Single-Cell Level

*Xiangxu Jiang, Ziyun Jiang, Tingting Xu, Shao Su, Yiling Zhong, Fei Peng, Yuanyuan Su, and Yao He**

Institute of Functional Nano & Soft Materials (FUNSOM) and Jiangsu Key Laboratory for Carbon-based Functional Materials & Devices, Soochow University, Suzhou 215123, China.

E-mail: yaohe@suda.edu.cn (Y. He)

SUPPORTING INFORMATION

Additional data

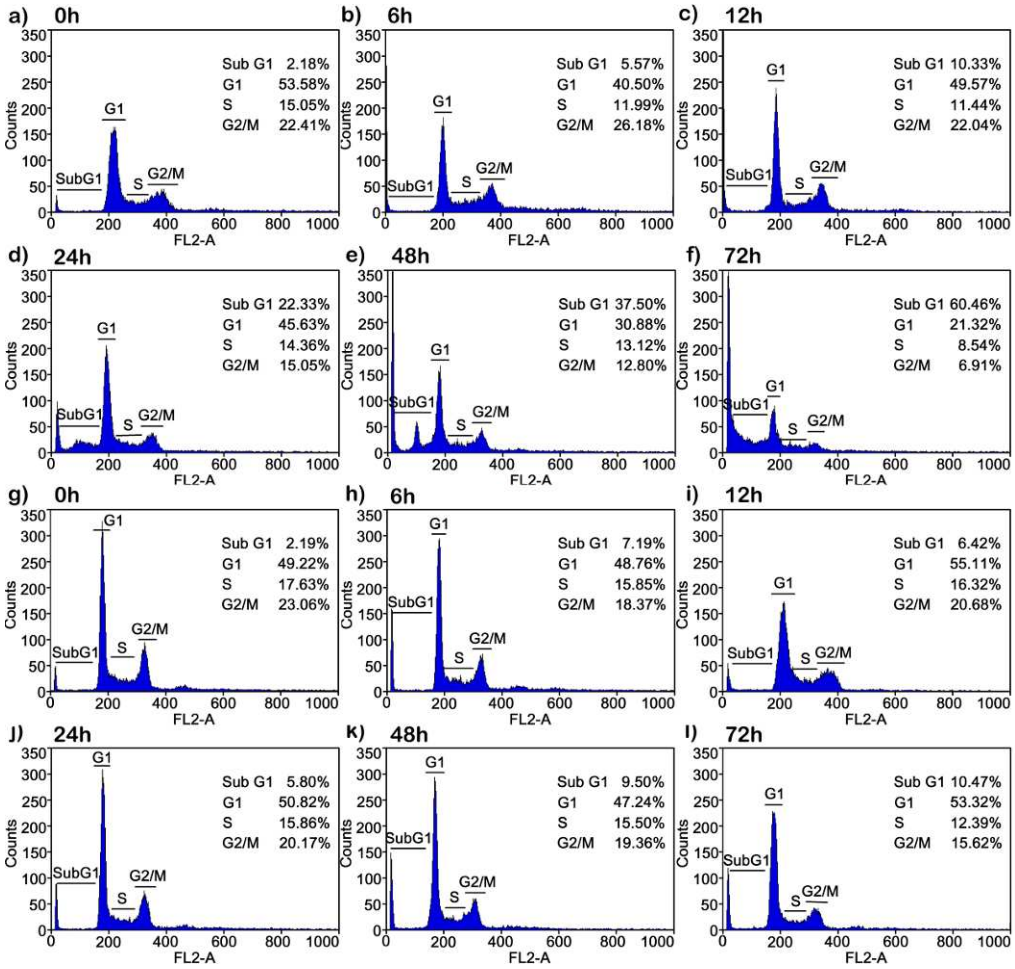

Figure S1. Corresponding flow cytometry analysis of AgNPs@Si-treated A549 cells cultured with a)-f) or without g)-l) apoptosis inducer (Triton X-100). Data on each sample represent the percentages of sub-G1, G1, S, and G2/M.

Propidium iodide (PI) staining detected by flow cytometry is carried out to quantitatively evaluate the apoptosis process of A549 cells (Figure S2).As is well known, the accumulation of the cells in Sub-G1 phase (the area left to the G0/G1 peak) is considered as a biomarker for DNA damage, and the appearance of this peak is related to the presence of apoptosis (e.g., apoptotic

cells with degraded DNA appeared in the Sub-G1 phase),[1-3] and PI dye is used to stain DNA after cells were fixed with cooled ethanol. As shown in Figure S1a-f, when A549 cells are cultured with both AgNPs@Si and apoptosis inducer, the cell number of the subG1 phase is 2.18 % at 0-h and increases to 5.57 % and 10.33 % after 6-and 12-h incubation time. Afterward, the number increases to 22.33%, 37.50 %, or 60.46 % when the incubated time is up to 24-, 48- or 72-h. In marked contrast, as A549 cells are cultured on the surface of AgNPs@Si alone, the cell numbers in subG1 area have feeble increase as incubation time ranging from 0 to 72 h (Figure S1g-l). These results further prove that apoptosis is basically not triggered by the AgNPs on the surface of silicon wafer, as the AgNPs are tightly immobilized on the surface and they could not enter into cells to induce undesirable effect on cells.[4-10]

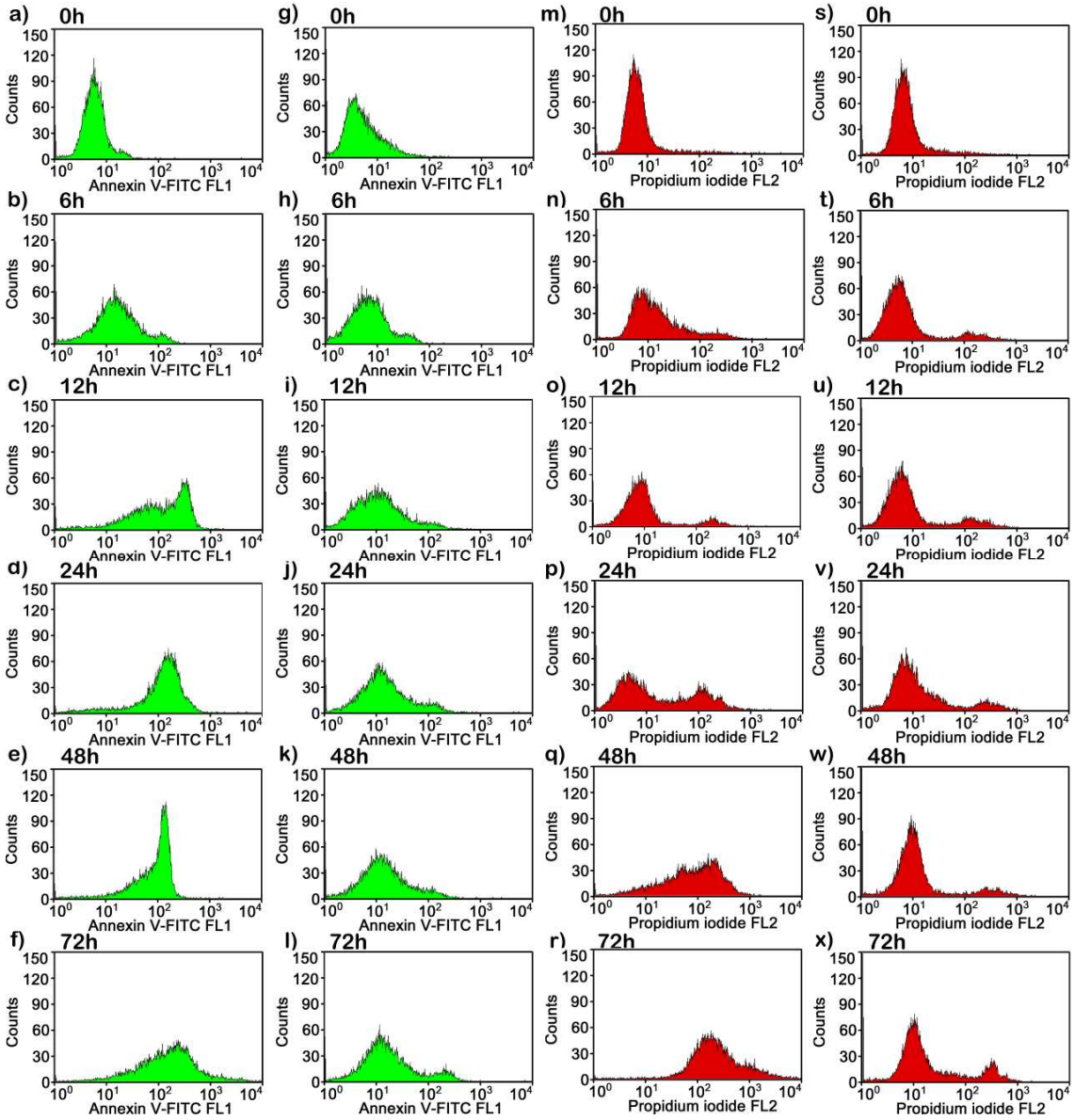

Figure S2. The flow cytometry histogram plots data of the live A549 cells treated with a)-f) or without g)-l) 150 μM Triton X-100 and stained with Annexin-V; the flow cytometry histogram plots data of the live A549 cells treated with m)-r) or without s)-x) 150 μM Triton X-100 and stained with PI.

After the cells treated with Triton X-100 for 0, 6, 12, 24, 48 and 72 h, the fluorescence intensities of the cells are tested by flow cytometry. The FITC fluorescence intensity increases obviously

when the incubation time is 12 h (Figure S2c), while no obvious fluorescence intensity increase is noted for PI at the same time (Figure S2o). As the incubation time increases (up to 24, 48 or 72 h) (Figure S2d-f, and p-r), both of the FITC and PI fluorescence intensity become stronger. By contrast, the fluorescence intensity of the control groups (without Triton X-100) has no evident change under the same conditions (Figure S2g-l and s-x). These results have fully demonstrated that the cells are under the early apoptotic stage after 12 h incubation, and gradually go into the late apoptotic stage, which is consistent with the Raman signals detected by AgNPs@Si-based SERS sensing platform (Figure 3a).

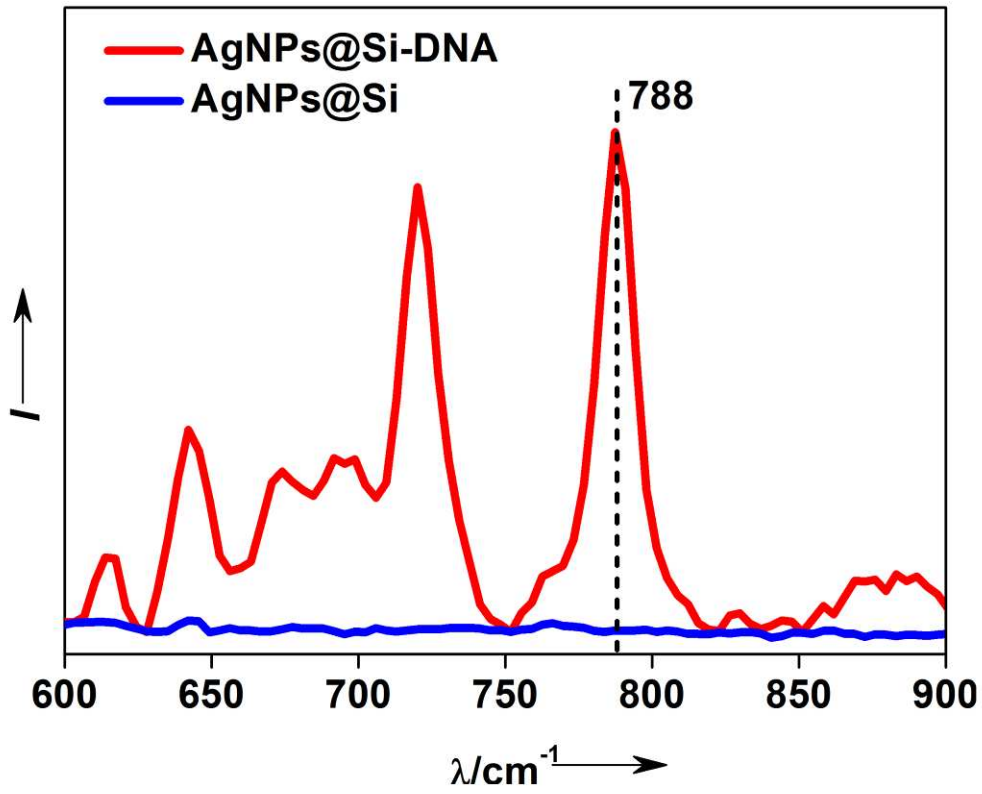

Figure S3. Raman spectra of the pure AgNPs@Si substrate without cells incubation (blue line), as well as DNA dispersed on the surface of the AgNPs@Si (red line). Note that, to guarantee objective comparison, DNA strands used for SERS detection are extracted for A549 cells. Notably, in comparison to feeble Raman intensities of pure AgNPs@Si, distinct Raman peak at 788 cm^{-1} is observed for DNA dispersed on the AgNPs@Si. It is well demonstrated that the 788 cm^{-1} Raman peak is ascribed to phosphodiester stretching of DNA and can be greatly enhanced by the AgNPs@Si, consisting with previous reports.[11,12]

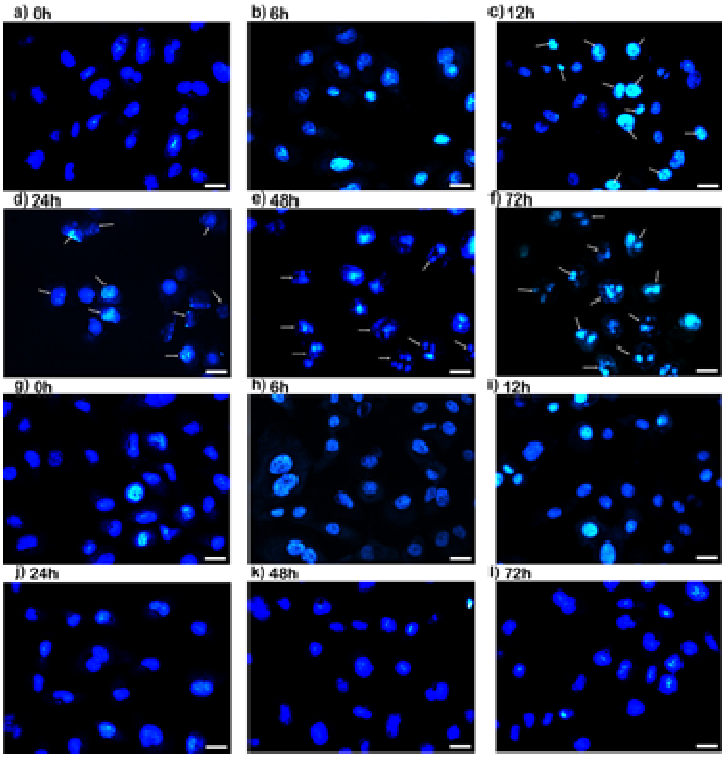

Figure S4. a-f) Fluorescence microscopy images show the apoptosis triggered by apoptosis inducer by staining the nucleus with Hoechst 33258 (excited by UV light and the emission is 405 nm). Arrows indicate DNA damage and chromatin condensation. g-l) As a control, AgNPs@Si-treated A549 cells in the absence of Triton X-100 are also stained and observed by the fluorescence microscopy. Scale bar = 25 μm.

In order to confirm the time course of the apoptotic cells, A549 cells treated with apoptosis inducer for different times are analyzed by fluorescence microscopy with Hoechst 33258 staining. As is well known, Hoechst 33258 is a specific DNA-binding fluorochrome, which binds preferentially to the A-T base pairs from the side of the minor groove of the DNA and can be used to visualize the apoptotic body formation and nuclear changes characteristic of apoptosis. [13-15] Figure S4 presents the confocal images of A549 cells stained by Hoechst 33258 after

incubation with apoptosis inducer for different times. Typically, cells show normal and round nucleus with a smooth nuclear membrane at 0-h incubation time (Figure S4a), while their nuclei diminish and the chromatin slightly condense when the incubation time increases to 6 h (Figure S4b). Afterwards, the chromatin becomes more condensed and shows a stronger blue-green fluorescence at 12-h incubation (Figure S4c), and starts to fragment at 24-h incubation (Figure 4d). The fragmentations of nucleus and chromatin are easily identified when the incubation time reaches 48 or 72 h (Figure S4e or 4f), respectively. Therefore, the observation of the fluorescence images demonstrates that the incubation of A549 cells with apoptosis inducer could result in gradually high apoptosis along with increasing incubation time, which is well consistent with the above-discussed SERS results. It is also of note that several studies reported that AgNPs inside cells via cellular uptake would induce apoptosis in some specific conditions, depending on size, concentration, surface modification, and cell types.[15] Thus, to avoid the possibility of AgNPs@Si-induced apoptosis, A549 cells cultured with AgNPs@Si alone are also evaluated as a control. As shown in Figure S4g-l, in the absence of apoptosis inducer, AgNPs@Si-treated cells show normal nuclei, with a smooth nuclear membrane, free of condensation and fragmentation. It indicates obvious apoptosis did not result from the AgNPs@Si, well consisting with the SERS results (Figures 3-5).

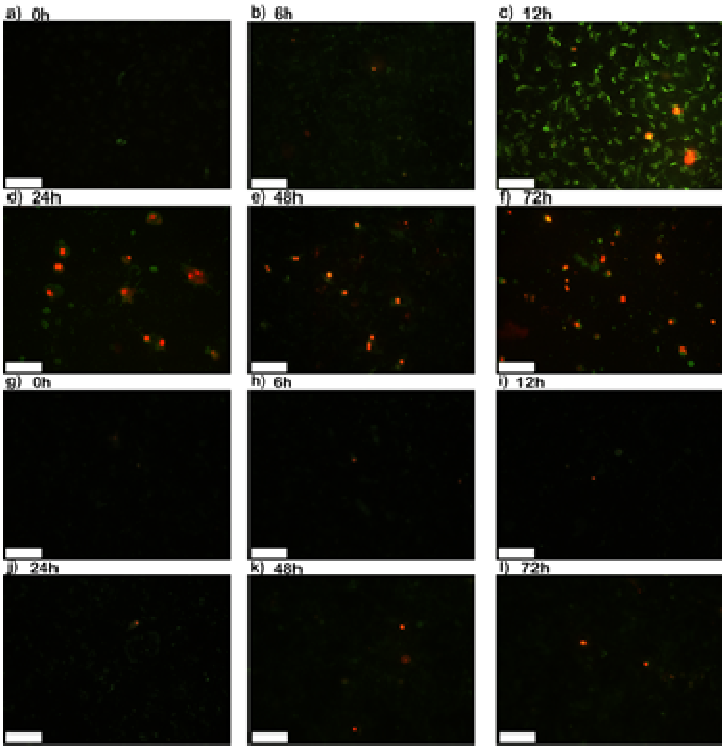

Figure S5. Fluorescence micrographs of live A549 cells stained with Annexin-FITC (green color) and PI (red color) treated with a-f) or without g-l) 150 μM Triton X-100. Scale bar = 50 μm.

The live-cell staining method is also performed to evaluate the apoptosis process of A549 cells, in which Annexin V conjugated to the fluorophor FITC and PI dyes are available to detect the apoptosis based on established protocols.[16,17] In brief, Annexin V which easily reacted with phosphatidylserin (PS) is used as a marker of apoptosis; while PI, which is utilized to detect plasma membrane integrity, is employed for recognizing necrotic cell death. As a result, unstained cells define viable cells; green or red fluorescent labels are classified as early apoptotic or necrotic cells, respectively, while dual stained cells are categorized as late apoptotic cells.[16,17] In our experiment, A549 cells treated with or without 150 μM Triton X-100 for different

incubation times (0, 6, 12, 24, 48 and 72 h) are visualized by fluorescence microscopy and flow cytometry (Figures S2 and S5). For Triton X-100 treated A549 cells, green Annexin-FITC fluorescence is increasingly intensified and reaches maximum value; meanwhile, only feeble red fluorescence of PI is detected, indicating the early stage of apoptosis triggered by the apoptotic inducer in the initial 12-h incubation (Figure S5a-c). With prolonged incubation from 24 to 72 h, both FITC (green) and PI (red) signals are clearly observed at the late stage of apoptosis (Figure 5d-f).[16] As a control, the cells cultured on AgNPs@Si surface but without apoptosis inducer treatment show weak signals of FITC and PI during 72-h incubation (Figure 5Sg-l). Similar phenomenon is also confirmed by flow cytometry (Figure S2). These results are well consistent with the SERS data (Figures 3-5), providing powerful demonstration that our SERS strategy is highly efficient for sensitive analysis of apoptosis at the single-cell level.

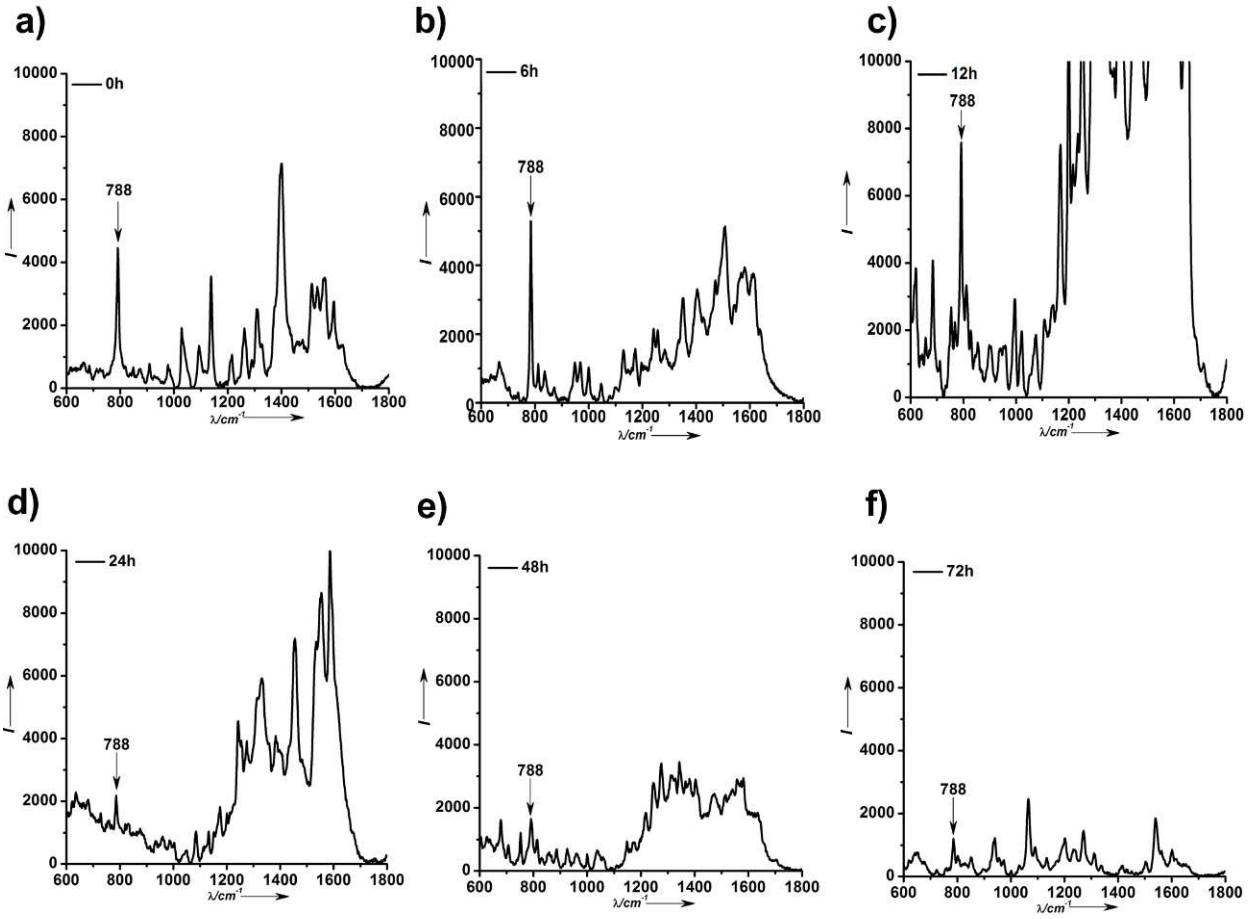

Figure S6. Raman spectra of the A549 cells treated with 150 μM Triton X-100 at the 0 h (a), 6 h (b), 12 h (c), 24 h (d), 48 h (e) and 72 h (f). Notably, despite interference of other biomolecules (e.g., protein, glucose, small molecules and others), 788 cm^{-1} Raman peak ascribed to phosphodiester stretching of DNA shows a specific and time-dependent alteration of SERS intensities. In particular, the A549 cell yields strong Raman signals (~ 4000) at 0-h incubation. At the early apoptosis stage for 6-h incubation, the SERS signals increase to a higher level (~5600), and reach the highest level (~10000) when the apoptosis time is up to 12 h. The SERS signals are significantly reduced to a low level (~2500) in the middle stage for 24 h, and further drop to ~1500 at 48 h, indicating an increasingly higher degree of apoptosis. With prolonging incubation time up to 72 h, the SERS signals dramatically drop to ~1000, revealing a remarkable apoptotic state of A549 cells.

REFERECCES

(1) Gao, Y.; Chen, L. L.; Zhang, Z. W.; Gu, W. W.; Li, Y. P. *Biomacromolecules* **2010**, *11*, 3102-3111.

(2) Wang, H. M.; Chiu, C. C.; Wu, P. F.; Chen, C. Y. *J. Agric. Food Chem.* **2011**,*59*, 8187-8192.

(3) Wlodkowic, D.; Faley, S.; Zagnoni, M.; Wikswo, J. P.; Cooper, J. M. *Anal. Chem*. **2009**, *81*, 5517-5523.

(4) He, Y.; Fan, C. H.; Lee, S. T. *Nano Today* **2010**, *5*, 282-295.

(5) He, Y.; Su, S.; Xu, T. T.; Zhong, Y. L.; Zapien, J. A.; Li, J.; Fan, C. H.; Lee, S. T. *Nano Today* **2011**, *6*, 122-130.

(6) Su, Y. Y.; Wei, X. P.; Peng, F.; Zhong, Y. L.; Lu, Y. M.; Su, S.; Xu, T. T.; Lee, S. T.; He, Y. *Nano Lett.* **2012**, *12*, 1845-1850.

(7) Braydich-Stolle, L.; Hussain, S.; Schlager, J. J.; Hofmann, M. C. *Toxicol. Sci.* **2005**, *88*, 412-419.

(8) Hussain, S. M.; Hess, K. L.; Gearhart, J. M.; Geiss, K. T.; Schlager, J. J. *Toxicol. In Vitro* **2005**, *19*, 975-983.

(9) Hussain, S. M.; Javorina, A. K.; Schrand, A. M.; Duhart, H. M.; Ali, S. F.; Schlager, J. J. *Toxicol. Sci*. **2006**, *92*, 456-463.

(10) Yen, H. J.; Hsu, S. H.; Tsai, C. L. *Small* **2009**, *5*, 1553-1561.

(11) Chan, J. W.; Lieu, D. K.; Huser, T.; Li, R. A. *Anal. Chem.* **2009**, *81*, 1324-1331.

(12) Jiang, Z. Y.; Jiang, X. X.; Su, S.; Wei, X. P.; Lee, S. T.; He, Y. *Appl. Phys. Lett.* **2012**, *100*, 203104.

(13) Liu, Z. S.; Tang, S. L.; Ai, Z. L. *World J. Gastroenterol* **2003**, *9*, 1968-1971.

(14) Dothager, R. S. K.; Putt, S.; Allen, B. J.; Leslie, B. J.; Nesterenko, V.; Hergenrother, P. J. *J. Am. Chem. Soc.* **2005**, *127*, 8686-8696.

(15) Wang, Y. L.; Chen, J. J.; Irudayaraj, J. *ACS Nano* **2011**, *5*, 9718-9725.

(16) Oh, W. K.; Kim, K.; Choi, M.; Kim, C.; Jeong, Y. S.; Cho, B. R.; Hahn, J. S.; Jang, J. *ACS Nano* **2010**, *9*, 5301-5313.

(17) Maher, S.; McClean, S. *Biochem. Pharmacol.* **2008**, *75*, 1104-1114.